# Three new approximations for estimation of $R_J$ from AVO

Charles P. Ursenbach


## ABSTRACT

Standard two-parameter inversion methods are analyzed and shown to be equivalent to each other below the critical point. New two-parameter methods are derived which are modifications of the method of Fatti et al. and which yield different estimates of the shear impedance reflectivity. The first is linear and its results can also be obtained by appropriate combination of the results of Fatti et al. The second is non-linear, containing a term quadratic in the shear impedance reflectivity, but it can be solved non-iteratively. Inversions of synthetic data are carried which show that these methods can improve on the Fatti method for large density and shear impedance reflectivities. Finally we demonstrate how to incorporate the quadratic term into estimation of shear impedance reflectivity from the intercept and gradient obtained from Shuey's two-term equation, and illustrate this with calculations on synthetic data.


## INTRODUCTION

In AVO inversion one seeks to determine earth-property contrasts across an interface from the angle-dependence of seismic amplitudes. The starting point is $R_{PP}(\theta_i)$, where $R_{PP}$ is the P-wave reflection coefficient determined from seismic amplitudes and $\theta_i$ is the angle of incidence at the interface. The final objective is a set of relative contrasts of the form $\Delta x/x$, which can also be expressed as reflectivities, $R_i$. We set out these definitions as follows:

$$\frac{\Delta x}{x} = \frac{x_2 - x_1}{(x_1 + x_2)/2} \qquad x = \alpha, \beta, \rho, I, J, \mu \qquad \gamma = \left(\frac{\beta_1 + \beta_2}{\alpha_1 + \alpha_2}\right)^2 \equiv \left(\frac{\beta}{\alpha}\right)^2$$

subscript 1 = earth layer above interface  subscript 2 = earth layer below interface

| | |
|---|---|
| $\alpha$ = P - wave velocity | $R_\alpha = (1/2)(\Delta\alpha/\alpha)$ |
| $\beta$ = S - wave velocity | $R_\beta = (1/2)(\Delta\beta/\beta)$ |
| $\rho$ = density | $R_\rho = (1/2)(\Delta\rho/\rho)$ |
| $I$ = P - wave impedance = $\rho\alpha$ | $R_I = R_\alpha + R_\rho$ |
| $J$ = S - wave impedance = $\rho\beta$ | $R_J = R_\beta + R_\rho$ |
| $\mu$ = shear modulus = $\rho\beta^2$ | $R_\mu = 2R_\beta + R_\rho$ |

The Aki-Richards approximation, a linearization of the Zoeppritz equations in $R_\alpha$, $R_\beta$, and $R_\rho$, has been the starting point for most AVO inversion work (Aki & Richards, 1980). While the Zoeppritz equations give exact coefficients for idealized transmission, reflection, and conversion events, their complicated structure necessitates the use of non-linear inversion techniques. Inversion with the Aki-Richards approximation is a one-step process, involving the least-squares solution of a set of linear equations.

In reality of course one requires some "background" parameters as input to the inversion. One requires an estimate of $R_\alpha$, for use in raytracing, and an estimate of $\gamma$. These are required to set up the coefficients in the Aki-Richards equation.

In practical inversions, the three-parameter Aki-Richards approximation is itself often set aside in favor of a two-parameter approximation. The best-known of these are the Smith-Gidlow approximation (Smith & Gidlow, 1987), in which a differential form of Gardner's relation (Gardner et al., 1974) is used to replace $R_\rho$ with $R_\alpha$, and the approximation of Fatti et al. (1994), in which the contribution of $R_\rho$ is assumed to be negligible in comparison to that of $R_I$ and $R_J$. The reason for reducing the number of parameters is that the presence of noise in the seismic data introduces large errors into the contrast estimates. Reducing the number of variables controls these errors. This is illustrated in Figure 1. Here we plot the results of inversion of synthetic data at 110 different interfaces. [This dataset (Castagna & Smith, 1994) and our use of it has been described in detail previously (Ursenbach, 2003a-d)]. When noise-free data is used, the Aki-Richards results are similar to those of the two-parameter methods. When noise is introduced however, the Aki-Richards results degrade rapidly relative to the two-parameter methods (except in prediction of $R_I$).

It should be noted that even when the two-parameter results are far better than the Aki-Richards results, they can still in absolute terms be much less accurate than is necessary to be useful.

In this research we develop three new AVO approximations. The first is a linear theory similar to the method of Fatti et al., but which has smaller errors in some situations. The second is a two-parameter method that is superior in some cases to the Fatti method for estimation of $R_J$. Although it is non-linear, it is unique in that it can be solved in a one-step process, without recourse to iterative techniques. The third is a method for incorporating non-linearity into the interpretation of intercept and gradient results.

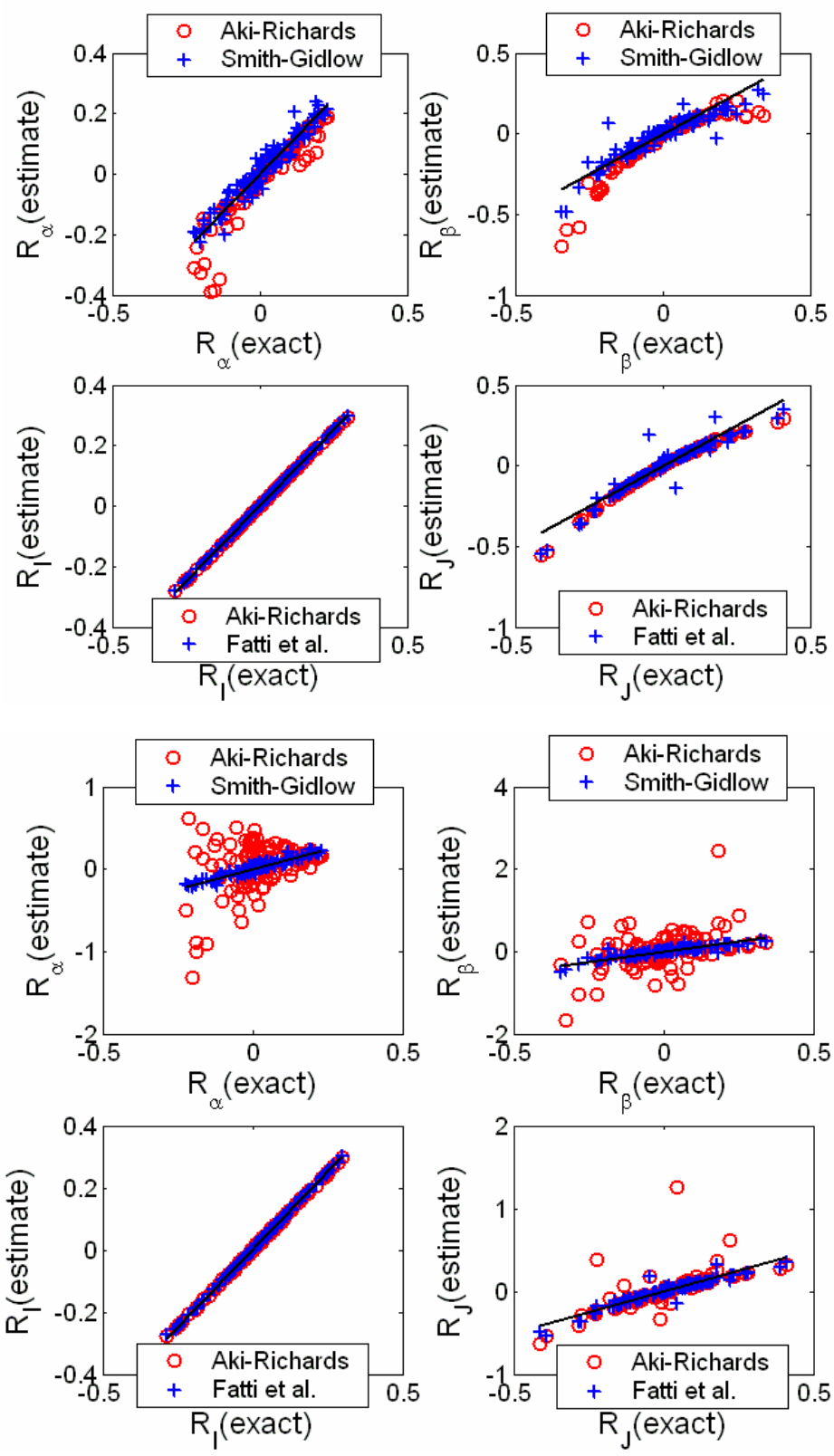


FIG. 1. In the top four panels inversion is carried out on noise-free data. The two- and three-parameter methods give similar results. Noisy data is used in the lower four panels, where two-parameter methods are much more accurate, except in the case of $R_I$.

## THEORY

### Linear two-parameter inversion with a simple two-data-point model, and a new approximation

To begin we first take a new look at what is actually being calculated in a two-parameter inversion. Consider a simple case involving only two offsets, one of which is zero. In this case the equations for a general two-parameter linear inversion can be written as

$$R_{PP}(0) = A_0 X + B_0 Y$$

$$R_{PP}(\theta_i) = A_1 X + B_1 Y$$

where $X$ and $Y$ are each some combination of reflectivities, and $A_i$ and $B_i$ are initially undetermined coefficients. To linear order, $R_{PP}(0) = R_\alpha + R_\rho$ and $R_{PP}(\theta_i) = R_\alpha/\cos^2\theta - 4\gamma \sin^2\theta\, R_\mu + R_\rho$ (as per the Aki-Richards equations, where $\theta = [\theta_i + \theta_t] / 2$, and $\theta_t$ is the P-wave transmission angle). The general solutions for $X$ and $Y$ will be linear combinations of $R_{PP}(0)$ and $R_{PP}(\theta_i)$. Thus they will also be linear combinations of $R_{PP}(0)$ and $\cos^2\theta R_{PP}(\theta_i) - R_{PP}(0)$. The latter choice is convenient because $R_{PP}(0)$ is independent of $R_\mu$ and $\cos^2\theta R_{PP}(\theta_i) - R_{PP}(0)$ is independent of $R_\alpha$. From the following arrangement of the general solution,

$$X = \frac{1/2}{A_0 B_1 - A_1 B_0}\left[\left(B_1 - \frac{B_0}{\cos^2\theta}\right)R_\alpha + 4B_0\left(\frac{\beta}{\alpha}\right)^2 \sin^2\theta R_\mu + \left(B_1 - B_0\right)R_\rho\right]$$

$$Y = \frac{1/2}{A_0 B_1 - A_1 B_0}\left[\left(\frac{A_0}{\cos^2\theta} - A_1\right)R_\alpha - 4A_0\left(\frac{\beta}{\alpha}\right)^2 \sin^2\theta R_\mu + \left(A_0 - A_1\right)R_\rho\right],$$

we see that this is equivalent to setting $B_0 = 0$ and $A_0/A_1 = \cos^2\theta$. The solutions then simplify to

$$X = (R_\alpha + R_\rho)/A_0 = R_I / A_0$$

$$Y = -\left(4\gamma \sin^2\theta R_\mu + \tan^2\theta R_\rho\right)/B_1$$

Any two parameter inversion will yield these two quantities or linear combinations thereof. An analysis of the method of Fatti et al. shows that it corresponds to $A_0 = 1/2$ and $B_1 = -4\gamma \sin^2\theta$, yielding

$$X(\text{Fatti}) = 2R_I \tag{1}$$

$$Y(\text{Fatti}) = R_\mu + \frac{R_\rho}{4\gamma\cos^2\theta} = 2R_\beta + \left(1 + \frac{1}{4\gamma\cos^2\theta}\right)R_\rho = 2R_J - \left(1 - \frac{1}{4\gamma\cos^2\theta}\right)R_\rho \tag{2}$$

Thus $Y$(Fatti) is, to linear order, strictly equal to $2R_J$ only when $\gamma \cos^2\theta = 1/4$. Analysis of the Smith-Gidlow method shows that

$$X(\text{S - G}) = \frac{8}{5}(R_\alpha + R_\rho) = \frac{8}{5}R_I = \frac{4}{5}X(\text{Fatti})$$

$$Y(\text{S - G}) = 2R_\beta + \frac{4R_\rho - R_\alpha}{5}\left(1 + \frac{1}{4\gamma\cos^2\theta}\right) = Y(\text{Fatti}) - \frac{X(\text{Fatti})}{10}\left(1 + \frac{1}{4\gamma\cos^2\theta}\right)$$

From these results we can see that the Smith-Gidlow $X$ and $Y$ are, to linear order, equal to $2R_\alpha$ and $2R_\beta$ if $R_\rho = R_\alpha/4$ (as per the Gardner relation). Furthermore the results of either the Fatti or Smith-Gidlow methods can be combined to obtain the results of the other.

Of course these theoretical results have been obtained assuming only two noise-free data points. In Figure 2 we present results obtained by least squares inversion on 31 noisy data points ($\theta = 0°, 1°, 2°, \ldots 30°$). We find that the conclusions above, with $\theta$ set to $\theta_{max}$, are still valid. Note that

$$\theta_{\max} = \frac{\theta_{i,\max} + \theta_{t,\max}}{2} = \frac{1}{2}\left(30^\circ + \sin^{-1}\left[\frac{1+R_\alpha}{1-R_\alpha}\sin 30^\circ\right]\right).$$

The only indication of an exception to total agreement is for $R_J$ estimates at the larger interface numbers. In this plot the interfaces are ordered according to their value of $R_\alpha$. Thus the points in question have the lowest critical points, and the lowest ones are in fact just above 30°. This is reasonable, as in the region well below the critical point (and for most interfaces of interest this means $\theta_{i,\max} < 30$), the reflectivity curve is well-described by two parameters, such as the intercept and gradient of Shuey's two-term approximation. This explains why the two-point model is successful below the critical point, but shows signs of breaking down as one approaches it.

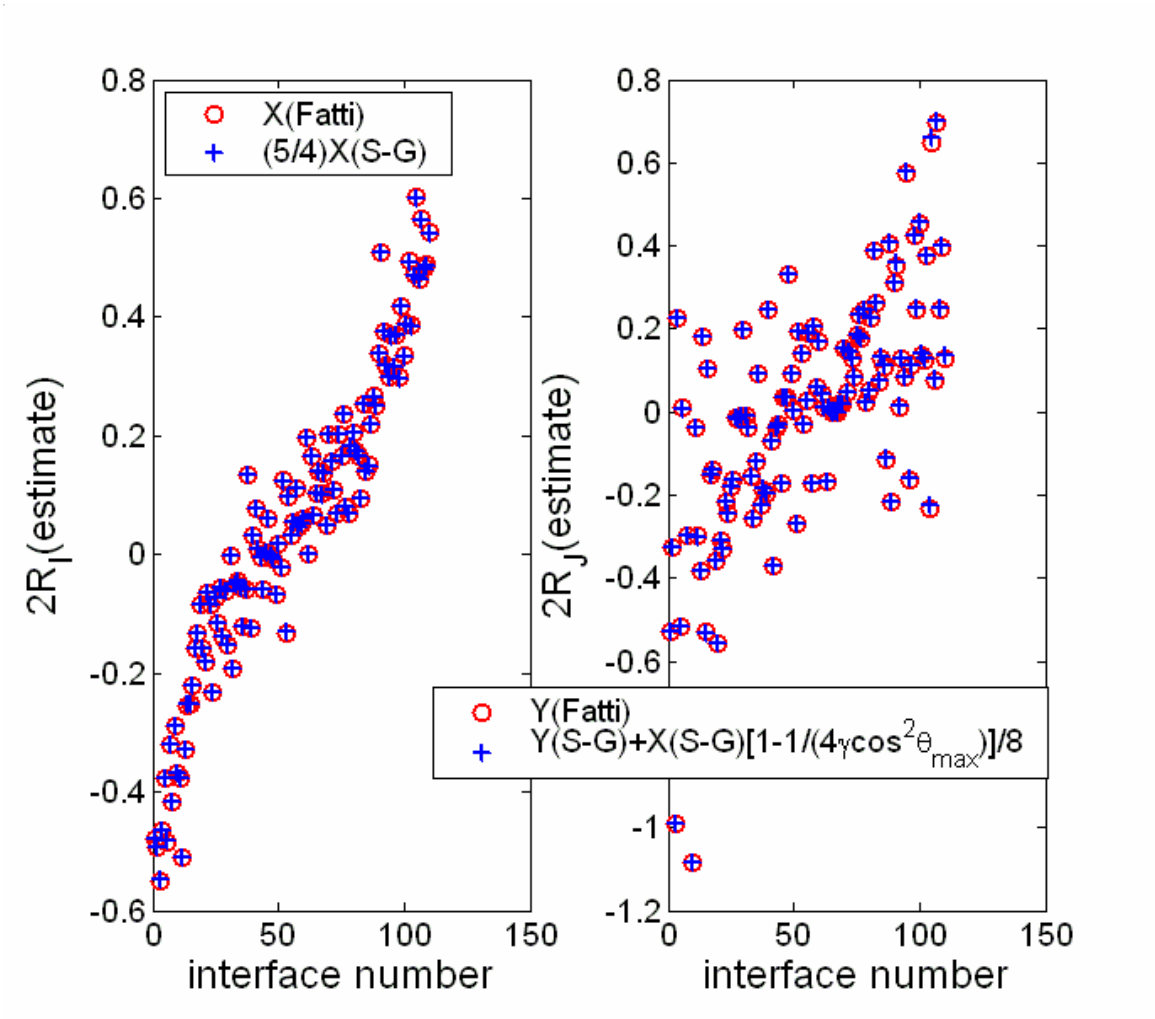


FIG. 2. A comparison showing that $R_I$ and $R_J$ estimates as calculated by the Fatti and Smith-Gidlow methods are equivalent. AVO inversion has been carried out by both methods on 110 interfaces, using data of Castagna and Smith (1994) as described in Ursenbach (2003a,b).

Thus the result of any two-parameter inversion can, to linear order and below the critical point, be reduced to Eqs (1) and (2). Eqn (1) of course is the P-impedance, but what is the quantity in Eqn (2)? It is some combination of $R_\beta$ and $R_\rho$, so in Figure 3 we compare it to $2R_\beta$, $2R_J$ and $R_\mu$. The closest correspondence is to $2R_J$, thus justifying its designation as such in the method of Fatti et al. This conclusion is further supported by the fact that there is a minus sign inside the third error term in Eq. (2), allowing for some cancellation. We denote $(1/2)Y$(Fatti) as $qR_J$, meaning "quasi-$R_J$". (We note however that Figure 3 was calculated with noise-free synthetic data, and that when noise is added, the three graphs look more similar.)

A better approach to estimating $R_J$ may be to approximate $R_\rho$ by $R_I/5$ and then obtain $R_J \cong Y(\text{S-G}) + X(\text{S-G})/4$. This can equivalently be obtained as

$$Y(\text{Fatti})+\frac{X(\text{Fatti})}{10}\left(1-\frac{1}{4\gamma\cos^2\theta}\right)=2R_J-\left(1-\frac{1}{4\gamma\cos^2\theta}\right)\frac{4R_\rho-R_\alpha}{5}\,. \qquad (3)$$

Comparing with Eq. (2) we see that this is the same as $Y$(Fatti) except that $R_\rho$ in the error term has been replaced by $(4\,R_\rho - R_\alpha)/5$. The latter quantity is generally smaller, at least for large $R_\rho$. This quantity can be obtained from Smith-Gidlow or Fatti results, or, because this is a linear theory, one can invert for it and $R_I$ directly using the same value of $B$ as in the Fatti method, but replacing $A$ by

$$A=\frac{1}{2\cos^2\theta}+\frac{1}{10}(4\gamma\sin^2\theta-\tan^2\theta)\,. \qquad (4)$$

Eq. (4) constitutes a new AVO approximation designed to give a more accurate estimation of $R_J$ for large $R_\rho$.

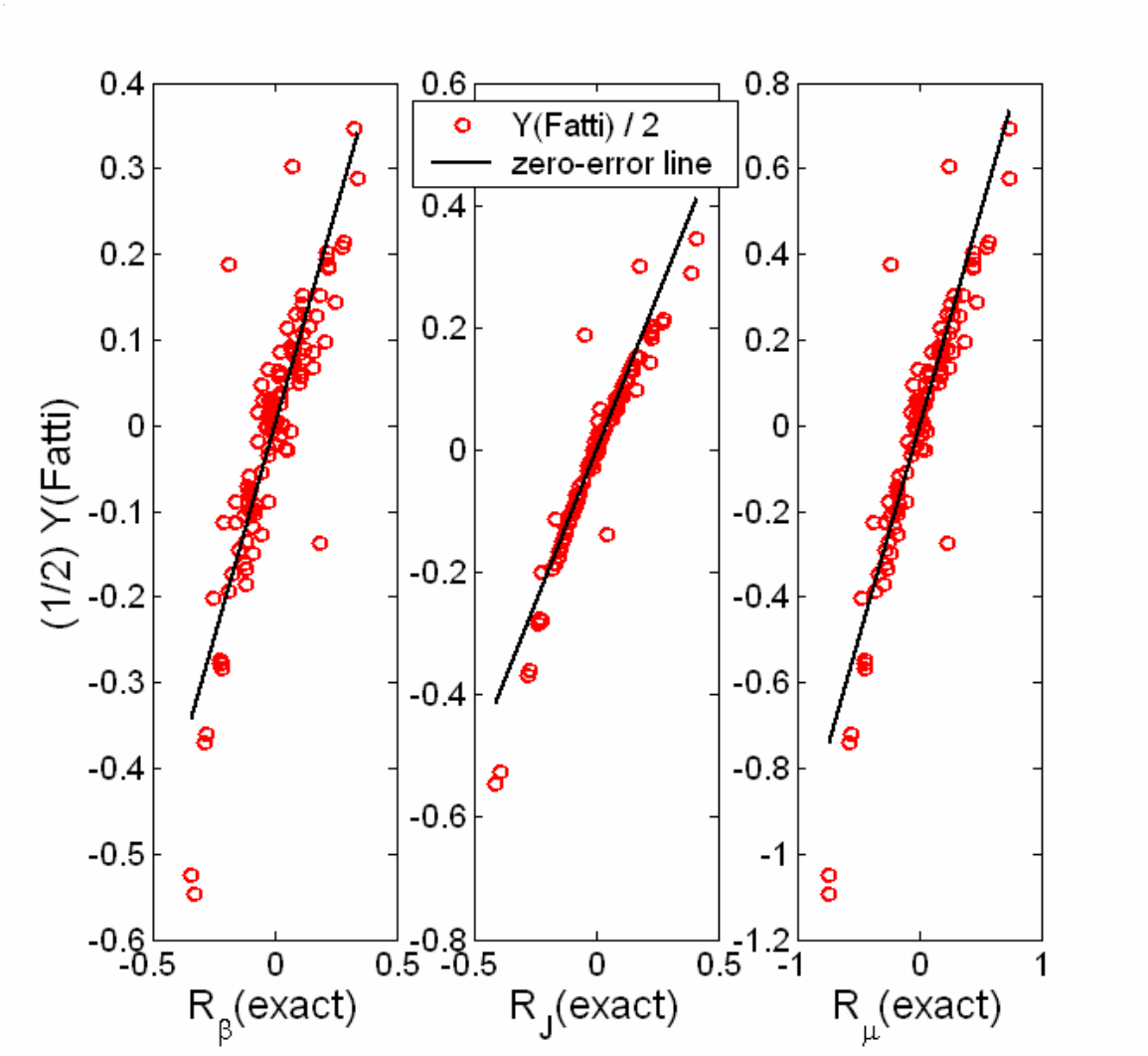


FIG. 3. The quantity of Eq. (2) obtained by Fatti AVO inversion is compared to $R_\beta$, $R_J$ and $R_\mu$ to see which it corresponds to the best. See Figure 2 for information on the data employed. The comparisons show that Eq. (2) most closely corresponds to $2R_J$.

### Importance of the $R_J^2$ term and the resulting AVO approximation

Armed with a detailed knowledge of $qR_J$, we might try using it to extract additional information. For instance, according to Eq. (2), we might try plotting $Y$(Fatti), calculated with different values of $\theta_{max}$, against $1/(4\gamma \cos^2\theta_{max})$ or against $1 + 1/(4\gamma \cos^2\theta_{max})$. This should yield a straight line with a slope of $R_\rho$ and an intercept of either $R_\mu$ or $2R_\beta$. However such attempts have been unsuccessful. The reason can be seen by plotting $R_J - qR_J$ against $R_\rho[1-1/(4\gamma \cos^2\theta)]$ and $R_J$ respectively, as shown in Figure 4. The abcissa of the first graph is the expected value for $R_J - qR_J$ based on the linear analysis in the previous section. One would then expect a straight line of slope 1 passing through the origin. However there are significant deviations, and in the second graph these are shown to be strongly correlated with $R_J^2$ (or $R_\beta^2$). These deviations obscure the linear $R_\rho$ trend, except at very large values of $R_\rho$.

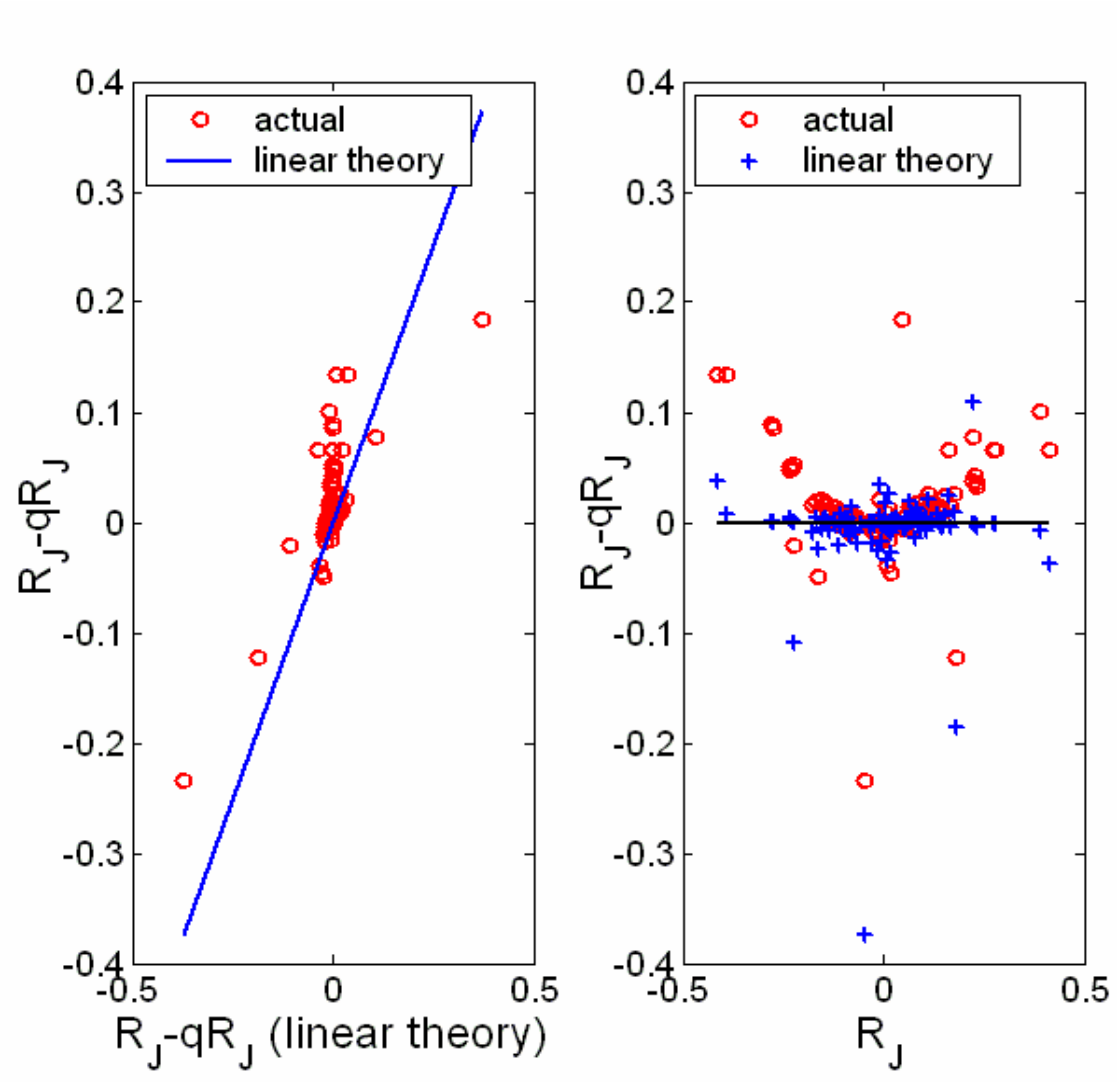


FIG. 4. According to the linear theory, $R_J - qR_J$ should be equal to $R_\rho[1-1/(4\gamma \cos 2\theta)]$. We plot these two quantities against each other, but in the first plot we see very poor agreement with linear theory predictions. The reason is clear in the second graph where the abscissa is changed to $R_J$. A strong correlation with $R_J^2$ is evident.

The results of Figure 4 motivate developing an AVO approximation of the form

$$R_{PP}(\theta) = A\frac{\Delta I}{I} + B_1\frac{\Delta J}{J} + B_2\left(\frac{\Delta J}{J}\right)^2. \tag{5}$$

A and $B_1$ can be assigned the same values as in the Fatti equation. $B_2$ can be obtained by using the methods described in Ursenbach (2003e) to formally derive the $(\Delta J/J)^2$ error term, and then choosing a value of $B_2$ which causes this term to vanish. The correct result which removes $(\Delta J/J)^2$ error terms in the inversion result is

$$B_2 = B_1\frac{\beta}{\alpha}\frac{\gamma\sin^2\theta - \cos^2\theta}{\cos\theta\cos\varphi} = B_1\frac{\beta}{\alpha}\frac{\sin^2\theta - \cos^2\varphi}{\cos\theta\cos\varphi} \tag{6}$$

where $\varphi$ is the average of converted-wave reflection and transmission angles at the interface. The quantity $\cos\varphi$ is, for this purpose, well approximated by $\sqrt{(1-\gamma\sin^2\theta)}$, and so requires no more input than that required by the linear theories.

Eq. (5) is a non-linear theory, so that the question of how to solve it is non-trivial. However it turns out that it can be solved exactly without resorting to iterative techniques. Seeking a least-squares solution, we obtain the Equations (7) and (8) below:

$$\left[\sum A_i^2\right]\frac{\Delta I}{I} = \left[\sum A_i R(\theta_i)\right] - \left[\sum A_i B_{1,i}\right]\frac{\Delta J}{J} - \left[\sum A_i B_{2,i}\right]\left(\frac{\Delta J}{J}\right)^2, \tag{7}$$

$$\begin{aligned}&\left[\sum A_i B_{1,i}\right]\frac{\Delta I}{I} + 2\left[\sum A_i B_{2,i}\right]\frac{\Delta I}{I}\frac{\Delta J}{J}\\ &\quad = \left[\sum B_{1,i} R(\theta_i)\right] + \left(2\left[\sum B_{2,i} R(\theta_i)\right] - \left[\sum B_{1,i}^2\right]\right)\frac{\Delta J}{J}\\ &\quad - 3\left[\sum B_{1,i} B_{2,i}\right]\left(\frac{\Delta J}{J}\right)^2 - 2\left[\sum B_{2,i}^2\right]\left(\frac{\Delta J}{J}\right)^3.\end{aligned} \tag{8}$$

Eq. (7) gives $R_I$ as a quadratic function of $R_J$. Substituting this expression for $R_I$ into Eq. (8) yields a cubic polynomial in $R_J$. This polynomial has three solutions to choose from, and $R_J$ is equal to the real root having the smallest magnitude. With $R_J$ known, $R_I$ can then be obtained explicitly from Eq. (7).

Eqs (5)-(8) constitute an augmented version of the Fatti method. Solution of this two-parameter theory will again yield the quantities of Eqs (1) and (2) as its results, but without the $R_J^2$ error apparent in Figure 4.

### Accounting for the $R_J^2$ term in the two-term Shuey approximation

We can obtain expressions analogous to Eqs (1) and (2) for the intercept and gradient obtained from the two-term Shuey approximation. It is useful though to add on a quadratic correction term based on Eqs (5) and (6). The result is

$$A = R_I, \tag{9}$$

$$\begin{aligned} B &= \frac{R_\alpha}{\cos^2\theta_{\max}} - 4\gamma\sin^2\theta_{\max}R_\mu - 16\gamma\sin^2\theta_{\max}\frac{\beta}{\alpha}\frac{\sin^2\theta_{\max}-\cos^2\varphi_{\max}}{\cos\theta_{\max}\cos\varphi_{\max}}R_J^2 \\ &\equiv \frac{R_\alpha}{\cos^2\theta_{\max}} - 4\gamma\sin^2\theta_{\max}R_\mu - 16\gamma\sin^2\theta_{\max}B_2^{\max}R_J^2, \end{aligned} \tag{10}$$

where $R$[Shuey] = $A$ + $B\sin^2\theta$, and $B_2^{\max}$ is implicitly defined in Eq. (10). This latter equation can be rearranged to

$$2B_2^{\max}R_J^2 + R_J - \left[\frac{A}{8\gamma\cos^2\theta_{\max}} - \frac{B}{8\gamma} - \left(\frac{1}{2} - \frac{1}{8\gamma\cos^2\theta_{\max}}\right)R_\rho\right] = 0. \tag{11}$$

If something can be done about the $R_\rho$ term, then this would provide a new method for predicting $R_J$ from $A$ and $B$. One choice is to set $R_\rho = 0$, which is reasonable as it is small, and there will be some cancellation in its coefficient. Another option is to apply Gardner's relation and set $R_\rho = R_I/5$. This yields

$$2B_2^{\max}R_J^2 + R_J - \left[\frac{A}{10\gamma\cos^2\theta_{\max}}\left(1 + \frac{1}{\gamma\cos^2\theta_{\max}}\right) - \frac{B}{8\gamma}\right] = 0. \tag{12}$$

We now have a quadratic polynomial in $R_J$, whose coefficients are determined by $A$, $B$, $\gamma$, and $\theta_{\max}$. The physical solution is given by

$$R_J = \frac{1 + \sqrt{1 + \left[\frac{4A}{5\gamma\cos^2\theta_{\max}}\left(1 + \frac{1}{\gamma\cos^2\theta_{\max}}\right) - \frac{B}{\gamma}\right]B_2^{\max}}}{4B_2^{\max}}. \tag{13}$$

We can compare the results of this to current methods of calculating $R_J$ from $A$ and $B$, such as

$$R_J = \frac{A - B}{8\gamma} \tag{14}$$

## APPLICATION

In this section we compare the abilities of different methods to accurately calculate $R_J$ with both noise-free and noisy data. We are not concerned with $R_I$ as it can be calculated with equal and high accuracy by all the methods. In all cases we carry out the inversion for 110 interfaces. This is similar to an inversion for 125 interfaces, described earlier (Ursenbach, 2003a-d), but with some systems deleted due to concerns over physicality.

We present the results for the 110 interfaces as [estimated $R$] – [exact $R$]. In the noisy cases we have added random noise to the P-P amplitudes.

Figure 5 shows that Eq. (3) (or Eq. (4)) does not affect the $R_J^2$ error, but that most of the outlying points (where the linear $R_\rho$ term is large) are improved.

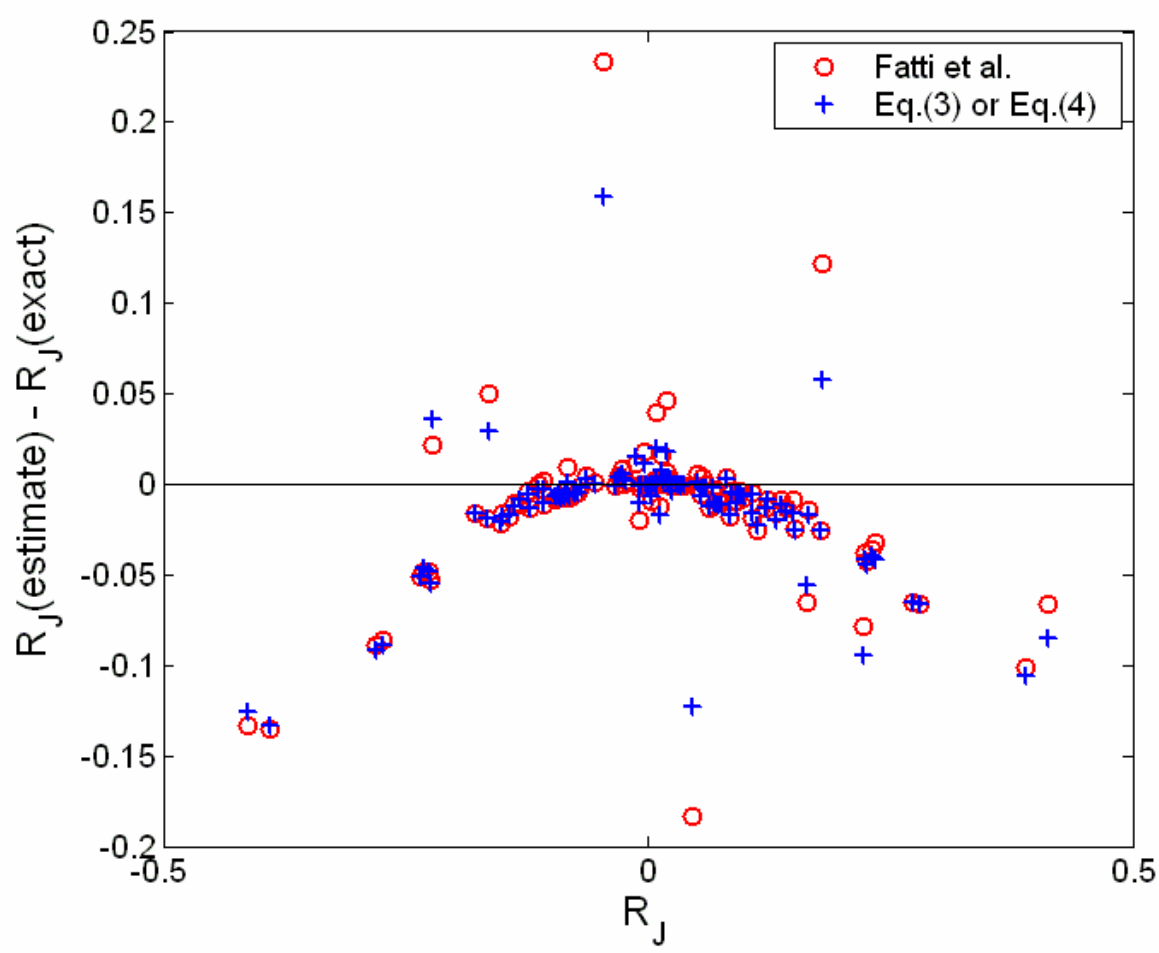


FIG. 5. A comparison of Fatti inversion with Eq. (4). Points away from the quadratic trend are associated with large linear $R_\rho$ error terms. When these errors are large, Eq. (4) reduces them by replacing $R_\rho$ by $0.8R_\rho - 0.2R_\alpha$ in the error term.

Figure 6 shows that Eq. (5) removes the $R_J^2$ errors from the $R_J$ estimates, and many of the outlying points are improved as well. Figure 7 shows that using Eq. (4) for the definition of $A$ in Eq. (5) is not equivalent to combining the results of Eq. (5) after the manner of Eq. (3). This is because Eq. (5) is a non-linear theory. Figure 7 also shows that the results of Eq. (5) are generally improved by applying Eq. (3) to them.

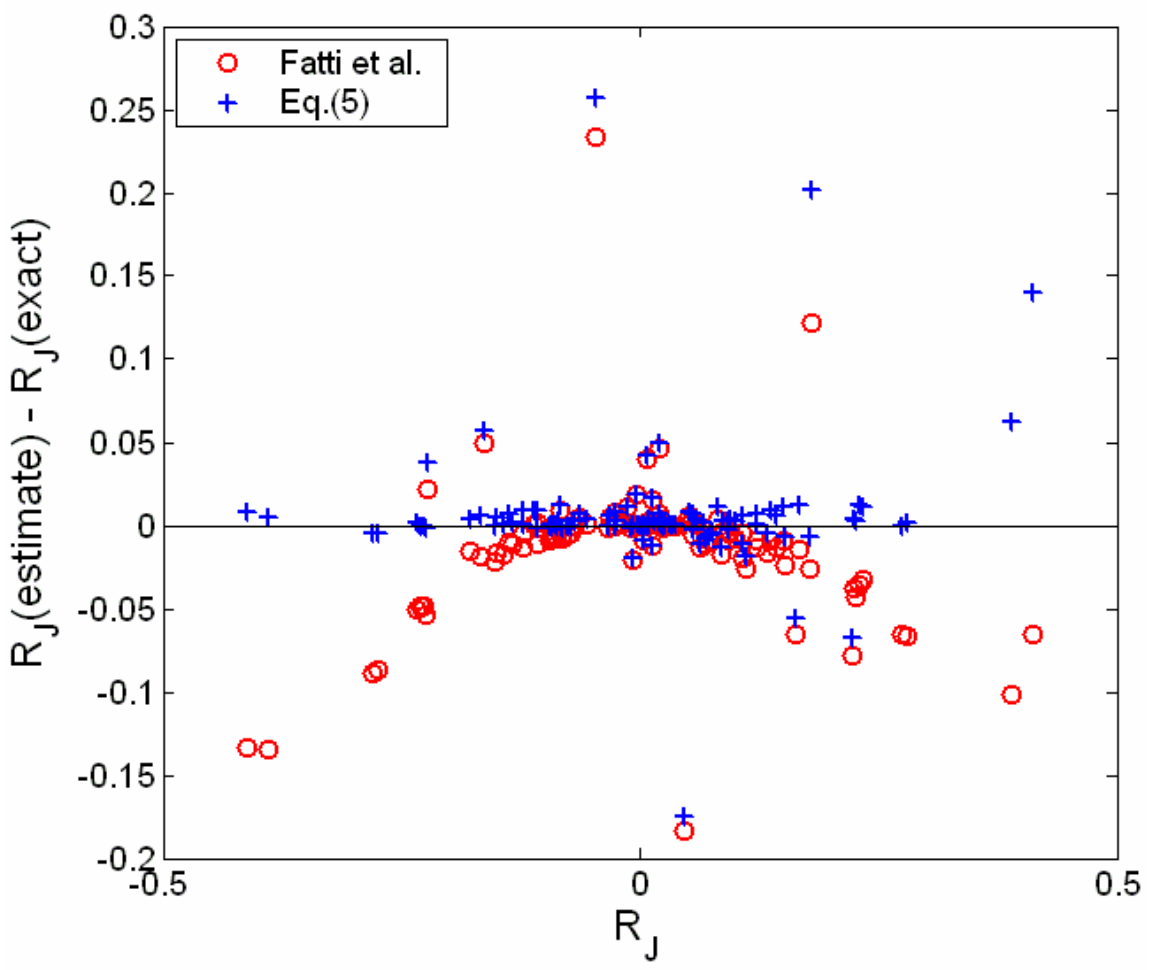


FIG. 6. A comparison of Fatti inversion with inversion based on Eq. (5). The $R_J^2$ error is clearly absent in the latter result. Errors associated with the linear $R_p$ term, represented by outlying points, are still present. However, many of the larger of such errors appear to be slightly improved.

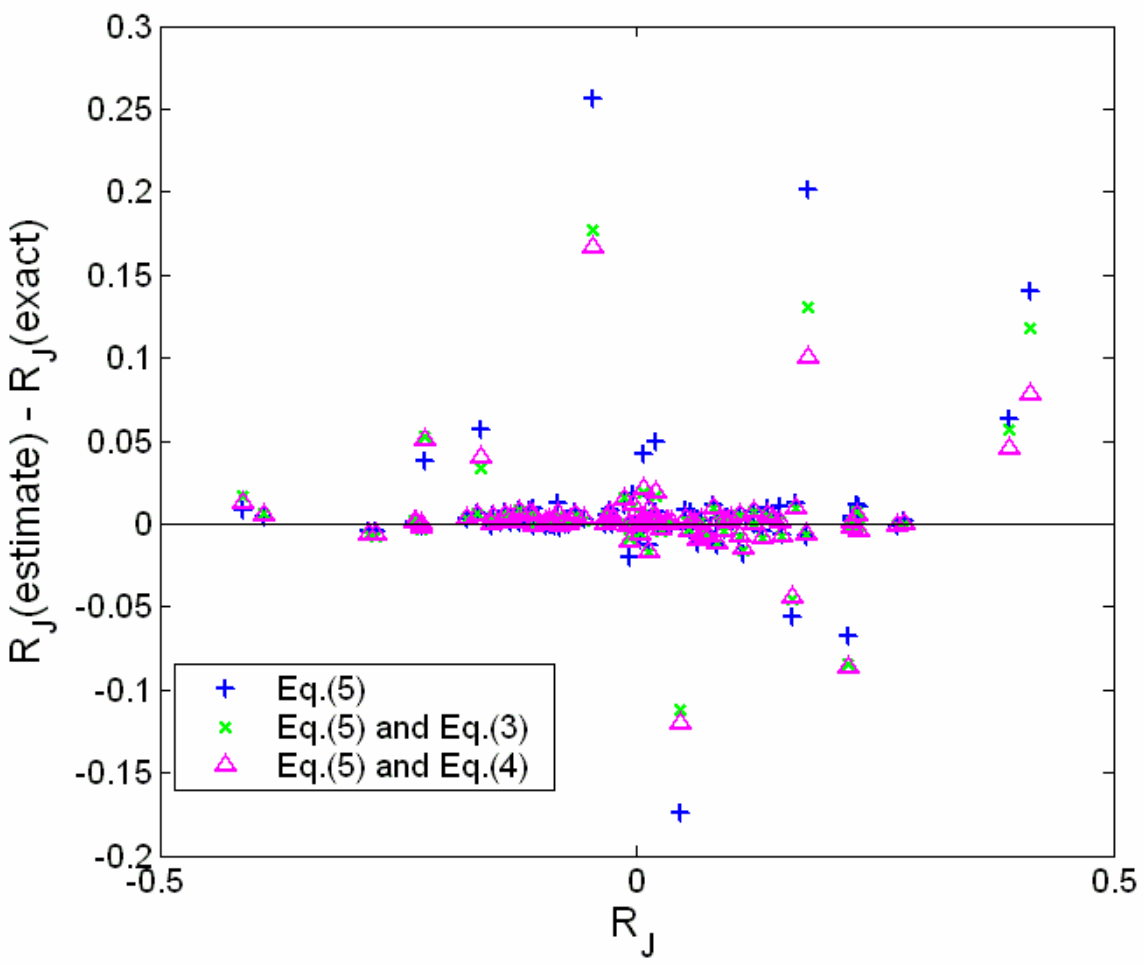


FIG. 7. A comparison of the method of Eq. (5) with two other methods derived from it. In one method the results of Eq. (5) inversion are combined in the manner of Eq. (3). In the other method the *A* parameter in Eq. (5) is defined by Eq. (4). For a linear theory these procedures would give identical results. Eq. (5) is non-linear, however, and use of Eq. (3) improves Eq. (5), while use of Eq. (4) degrades it. Eq. (5) should thus always be used with Eq. (3).

Figure 8 replicates the results of Figure 6, but with random noise added to the P-P amplitudes. One can still see similar trends, but the noise can potentially reverse the relative quality of the two methods for a given point. Figure 9 is instructive. We have found that the range of inversion errors induced by a given level of noise is inversely proportional to $\gamma$ and $\sin^2\theta_{max}$. Note that outlying points in the figures typically possess small $\gamma$. The non-linear theories are also proportional to $1+2R_\beta$, and the slope in both cases varies roughly as $\sqrt{(\theta_{i,max}/n)}$, where n is the number of data points (n=31 in Figures 1-8).

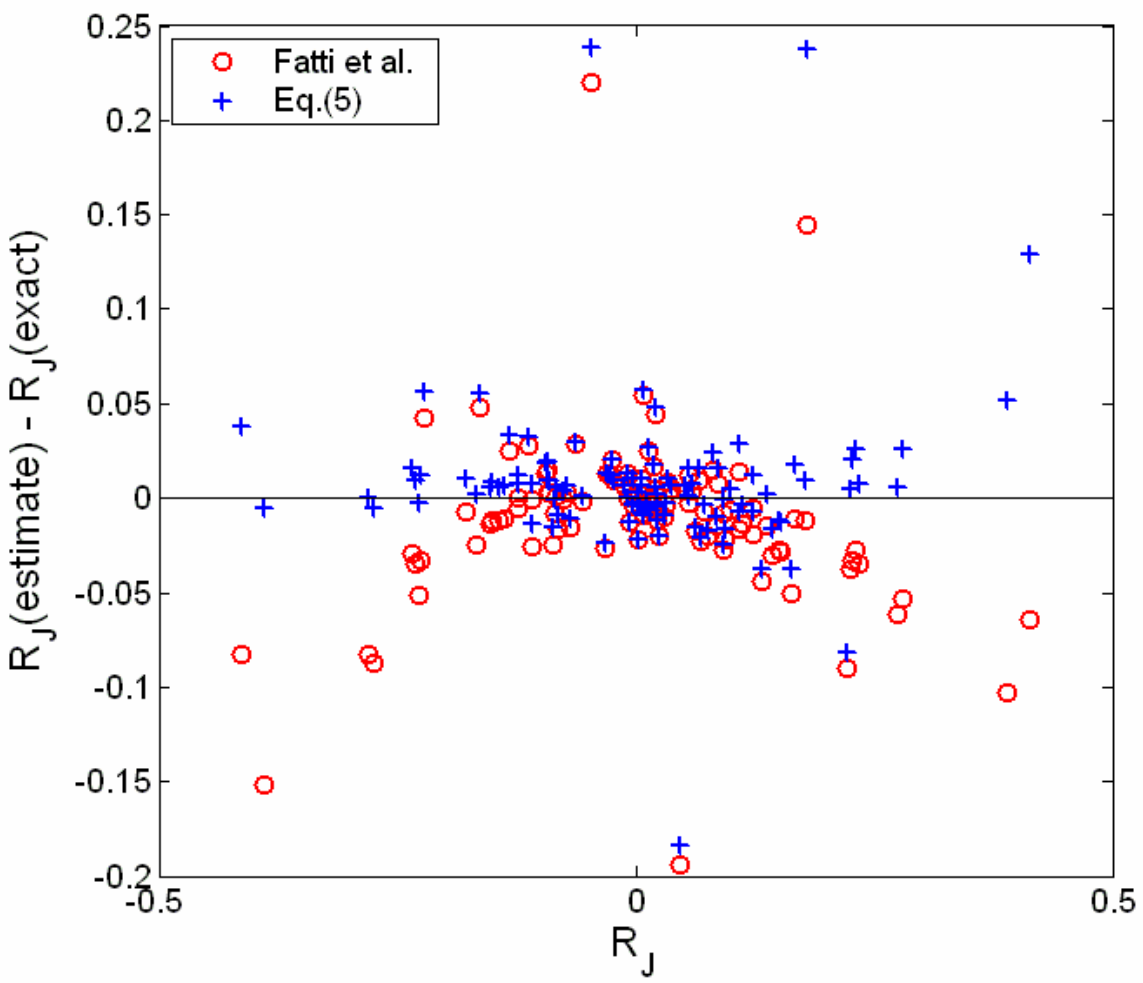


FIG. 8. This figure is identical to Figure 6 except that random noise has been added to the P-P amplitudes prior to inversion. The same trends can be discerned, but one can also see that with sufficient noise the order of quality of the two methods can be reversed for particular points.

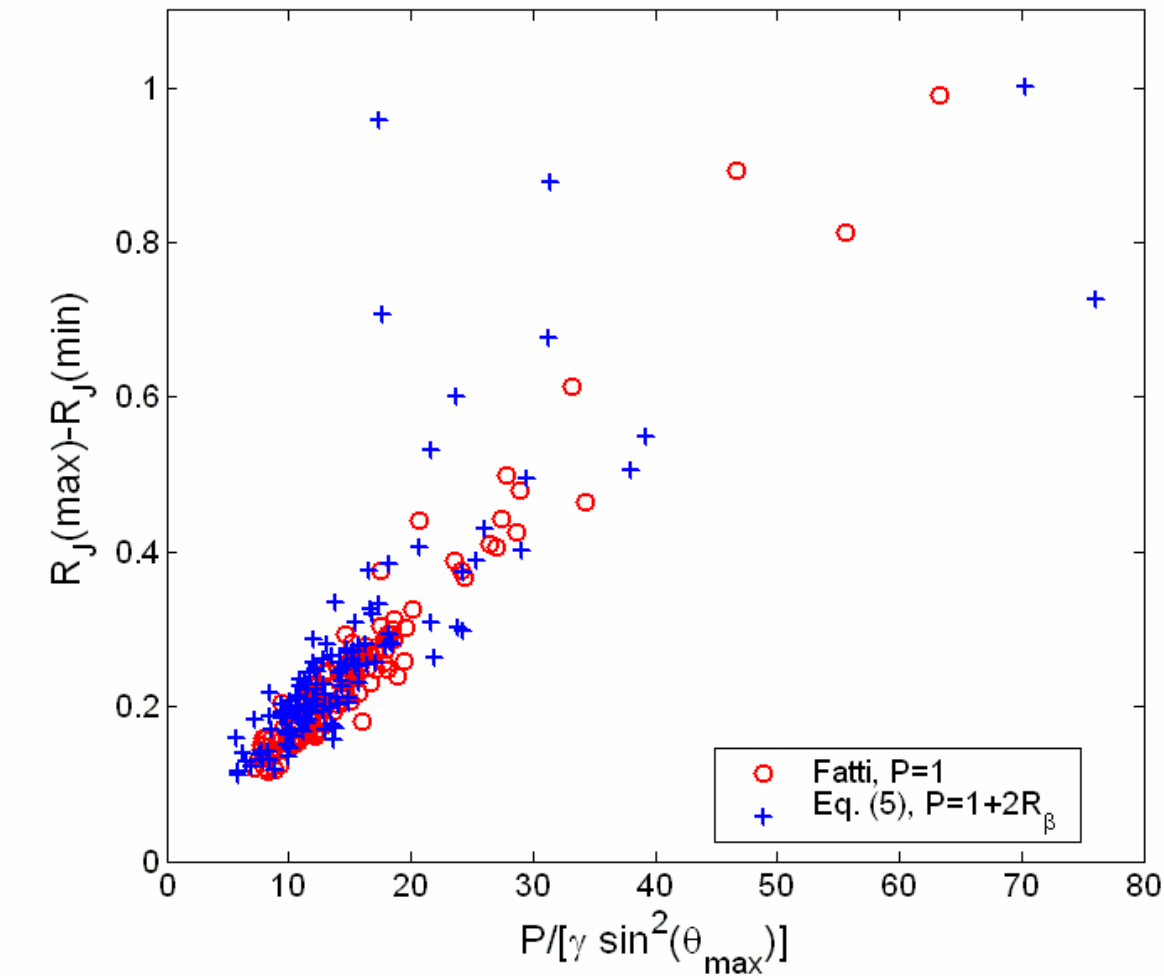


FIG. 9. To obtain this data, 100 inversions were carried out (for each of 125 interfaces) using different random errors each time. The value of $R_J$ predicted for each interface varied with the error used, and the difference of maximum and minimum predictions for each interface was obtained and plotted above. The range of predictions for each interface was found to correlate with $\gamma$ and $\sin^2\theta_{max}$, with a slope that depends on the interval between data points, and, for fixed $\theta_{i,max}$, varies as $1/\sqrt{n}$, where n is the number of data points. For quadratic methods, such as Eq. (5), the results also correlate with (1+ 2 $R_\beta$). Results from noisy data are distributed on both sides of the noise-free results, so the latter are a good indication of the average behavior of noisy data.

Finally we present results comparing the results of Eqs (13) and (14). These are shown in Figures 10. It is clear that Eq. (13) removes a quadratic trend that is present in the error of Eq. (14), and is generally superior for most values, except perhaps some with large density reflectivities.

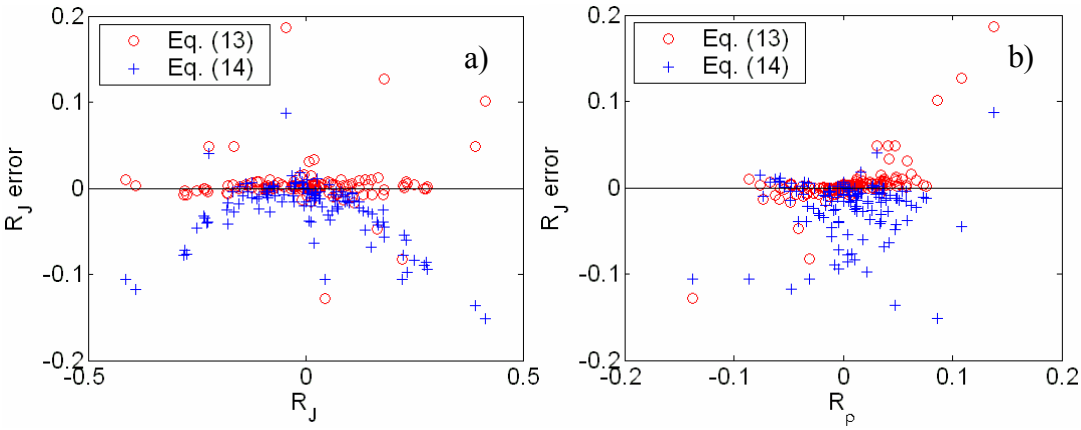


FIG. 10. A comparison of the errors in $R_J$ as predicted by Eqs (13) and (14). The results are plotted against the exact value of $R_J$ in a), where it is clear that Eq. (13) removes a quadratic trend from the error. The results are plotted against the exact value of $R_\rho$ in b), where it is seen that a few values predicted poorly by Eq. (13) are generally associated with interfaces possessing a large value of $R_\rho$.

## CONCLUSIONS

We have been able to demonstrate that the AVO methods of Smith-Gidlow and Fatti et al. (and all other linear, two-parameter methods) are equivalent in the subcritical region. Based on this we have developed an alternate linear AVO approximation which is more accurate when the true value of $R_\rho$ is large. We have also shown that, at least for noise-free data, the error quadratic in $R_J$ is usually larger than the error linear in $R_\rho$. Motivated by this result we have developed an augmented version of the Fatti method which includes a term quadratic in $R_J$. The new two-parameter method may be superior to the Fatti and Smith-Gidlow methods for calculation of $R_J$ and $R_\beta$ from noisy data when $R_J$ and $R_\beta$ are large, as long as $R_\rho$ is not too large also. Otherwise, the conventional methods may be preferable as they are simpler to calculate. This second method should always be used in combination with the first method, as that adds no extra difficulty and appears to give better results when $R_\rho$ is large. We have also shown that accounting for the quadratic term allows for better estimation of $R_J$ from the intercept and gradient of the two-term Shuey equation.

## REFERENCES

Aki, K. and Richards, P. G., 1980, Quantitative Seismology: Theory and Methods: W.H. Freeman, 1980.

Castagna, J. P. and Smith, S. W., 1994, Comparison of AVO indicators: A modeling study: Geophysics, **59**, 1849-1855.

Fatti, J. L., Smith, G. C., Vail, P. J., Strauss, P. J., and Levitt, P. R., 1994, Detection of gas in sandstone reservoirs using AVO analysis: A 3-D seismic case history using the Geostack technique: Geophysics, **59**, 1362-1376.

Gardner, G. H. F., Gardner, L. W., and Gregory, A. R., 1974, Formation velocity and density – The diagnostic basics for stratigraphic traps: Geophysics, **39**, 770-780.

Smith, G. C., and Gidlow, P. M., 1987, Weighted stacking for rock property estimation and detection of gas: Geophys. Prospecting, **35**, 993-1014.

Ursenbach, C., 2003a, Extension and Evaluation of Pseudo-Linear Zoeppritz Approximations: CSEG Extended Abstracts.

Ursenbach, C., 2003b, Can multicomponent or joint AVO inversion improve impedance estimates?: SEG Extended Abstracts.

Ursenbach, C., 2003c, Testing pseudo-linear Zoeppritz approximations: P-wave AVO inversion: CREWES 2003 Research Report.

Ursenbach, C., 2003d, Testing pseudo-linear Zoeppritz approximations: Multicomponent and joint AVO inversion: CREWES 2003 Research Report.

Ursenbach, C., 2003e, Testing pseudo-linear Zoeppritz approximations: Analytical error expressions: CREWES 2003 Research Report.

## ACKNOWLEDGMENTS

The author wishes to thank Jon Downton for discussions on limitations of the two-point model, and Bill Goodway for insights into the dataset employed.